

# A Pragmatic Labeling Design of MIMO BICM-ID Systems Based on EXIT Chart

Tsang-Wei Yu and Chung-Hsuan Wang  
Department of Communication Engineering,  
National Chiao Tung University,  
Hsinchu, Taiwan 30010, Taiwan

toshiba.cm93g@nctu.edu.tw and chwang@mail.nctu.edu.tw

Wern-Ho Sheen

Department of Information and Communication Engineering,  
Chaoyang University of Technology,  
Taichung County 41349, Taiwan

whsheen@cyut.edu.tw

**Abstract**—We propose a pragmatic labeling design based on the extrinsic information transfer (EXIT) chart for bit-interleaved coded modulation with iterative decoding on multiple-input-multiple-output channels. In our design, the EXIT chart is used to determine a candidate set of labelings which have representative demapper transfer curves. Then, a procedure to generate these labelings is provided based on the genetic algorithm. Given fixed channel code and signal-to-noise ratio (SNR), we can search within this candidate set for a most-suitable labeling to minimize the bit-error-rate (BER) with low complexity. Simulation results show that the labeling chosen from the candidate set exhibits a controllable BER performance gap compared to the optimal labeling found through exhaustive search. Besides, even though the channel code or the SNR is changed, the same candidate set can still be directly adopted to reduce the time on re-searching a new labeling.

## I. INTRODUCTION

Bit-interleaved coded modulation with iterative decoding (BICM-ID) [1][2] has been shown as an efficient and powerful transmission scheme over fading channels. It was pointed out in [1][2] that different BER performance can be obtained by employing different labelings. Recently, various researches have been done to find out good labelings of the BICM-ID systems for single-input-single-output (SISO) channels [3][4]. For multiple-input-multiple-output (MIMO) channels, single-dimensional labelings are investigated in [5][6], while [7][8] consider more general cases, called multi-dimensional labelings. Part of these works adopt the assumption of error-free feedback from the decoder and the labelings obtained turn out to have good BER performance at high signal-to-noise ratios (SNRs) but experience unacceptable performance loss at low or moderate SNRs.

In fact, it was mentioned in [4] that for any SNR the suitability of a labeling can always be determined with the help of the extrinsic information transfer (EXIT) chart [9], which has been known to be a powerful tool to understand the convergence behavior of iterative decoding schemes. Given a channel code and a fixed SNR, a good labeling should have the information transfer curve of demapper that makes a high first intersection with the decoder curve to allow the trajectory to go as far as possible. However, since any changes of the channel code and SNR may result in variations on the decoder and demapper curves respectively, the desired labeling should

also be different. An intuitive way to keep the optimality is to exhaustively plot the demapper curves of all possible labelings on the EXIT chart to find a new one whenever the channel code or SNR is changed. Obviously, the complexity of such an exhaustive search turns out to be infeasible, especially for large number of transmit antennas and large constellations. To reduce the search complexity, the binary switch algorithms (BSA) are employed in [4] for labeling searching.

In this paper, a pragmatic methodology for labeling design is presented to accommodate the impact of different channel codes and SNRs. Based on the EXIT chart, an observation shows that for the demapper transfer curves that have similar shapes and similar values on their left and right end points, their corresponding behavior on the BER performance, including the occurrence of the waterfall region and the BER of the error floor region, are usually similar [10]. Therefore, we can first partition all possible labelings into groups according to their values of two end points and then choose a representative labeling from each group to form a set, called the candidate set. As long as the channel code and SNR are given, we can search within the candidate set for a most-suitable labeling with low search complexity. To practically generate the candidate set, a procedure is proposed based on the genetic algorithm (GA) [11]. Simulation results show that the labeling we chosen from the candidate set can exhibit a controllable BER performance gap compared to the optimal labeling found through exhaustive search. Besides, even though the channel code or the SNR is changed, the same candidate set still can be directly adopted to reduce the time on re-searching a new labeling.

The rest of this paper is organized as follows. In Section II the system model of MIMO BICM-ID is given as well as the basic guideline of labeling design based on the EXIT chart. The idea of the candidate set and the procedure for generating the set are presented in Section III. In Section IV, simulation results are provided to verify the validity of our design for different channel codes and SNRs. Finally, a conclusion is drawn in Section V.

## II. SYSTEM MODEL AND EXIT CHART BASED ANALYSIS

Consider the system model of MIMO BICM-ID with  $N_T$  transmit antennas and  $N_R$  receive antennas as shown in Fig.

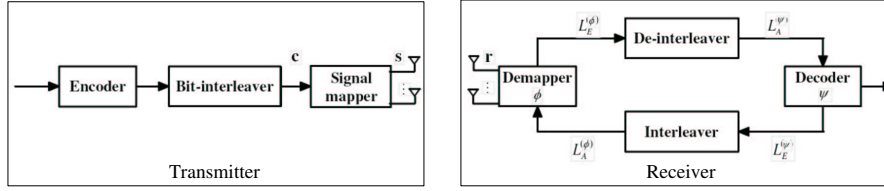


Fig. 1. Block diagram of BICM-ID systems.

1. A binary sequence  $\mathbf{c} = [c_0, \dots, c_{mN_T-1}]$  generated by an encoder  $C$  and an interleaver is first mapped to a vector  $\mathbf{s} = [s_1, \dots, s_{N_T}]^T$  by a labeling  $\mu$ , where  $s_n$  is drawn from a regular constellation  $\chi$  with  $2^m$  signal points,  $\forall 1 \leq n \leq N_T$ . For single-dimensional labelings,  $\mathbf{c}$  is first partitioned into  $N_T$  groups and then each group is mapped to a scalar signal point  $s_n$  before de-multiplexed to transmit antennas. Here, we consider multi-dimensional labelings [7] which directly map  $\mathbf{c}$  to  $\mathbf{s}$ . The signal vector  $\mathbf{s}$  is then transmitted through a frequency-nonselective MIMO channel, and the received signal  $\mathbf{r} = [r_1, \dots, r_{N_R}]^T$  can be expressed as

$$\mathbf{r} = \mathbf{H}\mathbf{s} + \mathbf{w}, \quad (1)$$

where the channel gain  $\mathbf{H}$  is an  $N_R \times N_T$  matrix with each element being identical independent complex Gaussian distribution of zero mean and unit variance and the noise  $\mathbf{w}$  is an  $N_R \times 1$  vector in which the elements are zero-mean complex Gaussian random variables with variance  $N_0/2$  per dimension.

The receiver is divided into two main blocks: the demapper and the decoder. Upon receiving  $\mathbf{r}$ , the demapper  $\phi$  takes  $\mathbf{r}$  as well as  $L_A^{(\phi)}(c_i)$ 's, the a priori inputs of coded bits feedback from the decoder  $\psi$  to compute the extrinsic log-likelihood ratios (LLRs)  $L_E^{(\phi)}(c_i)$ 's according to

$$L_E^{(\phi)}(c_i) = \ln \frac{\sum_{s \in \kappa_i^1} \exp \left\{ -\frac{\|\mathbf{r} - \mathbf{H}\mathbf{s}\|^2}{N_0} + \sum_{j \neq i} c_j L_A^{(\phi)}(c_j) \right\}}{\sum_{s \in \kappa_i^0} \exp \left\{ -\frac{\|\mathbf{r} - \mathbf{H}\mathbf{s}\|^2}{N_0} + \sum_{j \neq i} c_j L_A^{(\phi)}(c_j) \right\}}, \quad (2)$$

where  $\kappa_i^0$  and  $\kappa_i^1$  denote the sets consisting of all the  $\mathbf{s}$ 's for which the corresponding  $c_i$  is of binary value 0 and 1, respectively. These extrinsic outputs of demapper are then de-interleaved and taken by the decoder as the a priori inputs  $L_A^{(\psi)}(c_i)$ 's. By an appropriate soft-input soft-output decoding algorithm, e.g. the BCJR algorithm [12], the decoder generates the extrinsic LLRs  $L_E^{(\psi)}(c_i)$ 's and passes them back to the demapper for further iterations of decoding.

To trace the effect of  $\mu$  on MIMO BICM-ID, we use the EXIT chart for performance analysis on account of its iterative processing nature. By evaluating the mutual information between LLRs and the coded bits, two information transfer curves  $\Phi_\mu(\cdot)$  and  $\Psi_C(\cdot)$  are plotted in the EXIT chart to describe how the input information  $I_A^{(\phi)}$  and  $I_A^{(\psi)}$  are transferred to the output information  $I_E^{(\phi)}$  and  $I_E^{(\psi)}$  by the demapper  $\phi$  and decoder  $\psi$  respectively, i.e.

$$I_E^{(\phi)} = \Phi_\mu(I_A^{(\phi)}) \quad \text{and} \quad I_E^{(\psi)} = \Psi_C(I_A^{(\psi)}). \quad (3)$$

Note that  $\Phi_\mu(\cdot)$  is also a function of the SNR, though we omit the corresponding parameter of SNR for simplicity. We also define the two end points of the demapper curve by

$$\alpha_\mu = \Phi_\mu(0) \quad \text{and} \quad \beta_\mu = \Phi_\mu(1). \quad (4)$$

Let  $p_{\mu,C}$  denote the first intersection of the demapper and decoder curves, i.e. the smallest mutual information that makes  $\Phi_\mu(I) = \Psi_C^{-1}(I)$ . According to the EXIT chart, the BER of BICM-ID systems after a sufficient iterations is determined by  $p_{\mu,C}$ . Since a labeling that achieves a higher value of  $p_{\mu,C}$  is able to provide a lower BER, intuitively, one can always obtain a labeling which can achieve the lowest BER by exhaustive search such that

$$\mu_C^* = \arg \max_{\mu \in U} p_{\mu,C}, \quad (5)$$

where  $U$  denotes the set of all possible labelings.

### III. PRAGMATIC DESIGN METHODOLOGY OF LABELING WITH LOW SEARCH COMPLEXITY

The exhaustive search in (5) can always guarantee the lowest BER at a fixed channel code and a fixed SNR. However, since the decoder curve depends on the channel code and the demapper curve varies with the SNR, to the best of our knowledge there does not exist an universal labeling of regular modulation that is optimal for all channel codes and SNRs. An intuitive way to keep the optimality is to perform (5) whenever the channel code or the SNR is changed. Obviously, the corresponding search complexity becomes infeasible as  $m$  or  $N_T$  increases. Although algorithms, such as BSA, can be used to speed up the search time, the resulting complexity is still high if the channel code or the SNR is changed frequently. Besides, given fixed channel code and SNR, we observe that the labelings with similar values of  $\alpha_\mu$ 's and  $\beta_\mu$ 's, will usually have similar BER performance. (Here, the BER performance includes the SNRs where the waterfall regions occur and the BERs of the error floor regions.) Therefore, we may be able to perform a more efficient search if we can avoid trying the demapper curves with similar shapes.

Motivated by above two reasons, an intuitive idea is to first partition all possible labelings into  $N$  groups according to the similarity of their  $\alpha_\mu$ 's and  $\beta_\mu$ 's. Then one representative labeling is picked from each group to form a set of labelings, call the candidate set  $\Gamma$ . Once the channel code and the SNR are known, the labeling can then be selected within  $\Gamma$  by

$$\mu_C^\Gamma = \arg \max_{\mu \in \Gamma} p_{\mu,C}. \quad (6)$$

In this way, we can both reduce the search complexity by controlling  $N$ , the number of labelings in  $\Gamma$ , and avoid trying demapper curves with similar shapes. However, it is infeasible to plot the demapper curves of all possible labelings on the EXIT chart, especially for large  $m$  and  $N_T$ . Therefore, to obtain  $\Gamma$  in practice, we would like to first determine the desired values of  $\alpha_\mu$ 's and  $\beta_\mu$ 's we need in  $\Gamma$ , and then find corresponding labelings to approach these values. Let  $\mu_0$  denotes the Gray labeling, which is known as the one with the largest  $\alpha_\mu$  and smallest  $\beta_\mu$  among all labelings. Now the procedure for generating  $\Gamma$  is listed as following:

**Procedure for generating  $\Gamma$ :**

- Step 1: Use GA to find the labeling with the largest  $\beta_\mu - \alpha_\mu$ . Denote this labeling by  $\mu_{N-1}$  and let  $n = 0$ .
- Step 2: Let  $\delta_\alpha = \frac{\alpha_{\mu_0} - \alpha_{\mu_{N-1}}}{N-1}$  and  $\delta_\beta = \frac{\beta_{\mu_{N-1}} - \beta_{\mu_0}}{N-1}$ . Let  $\alpha_k^* = \alpha_{\mu_0} - k * \delta_\alpha$  and  $\beta_k^* = \beta_{\mu_0} + k * \delta_\beta$ ,  $\forall k = 1, 2, \dots, N - 2$ .
- Step 3: Let  $n = n + 1$  and use GA to find the labeling  $\mu_n$  that minimizes the fitness function  $\theta_n(\mu)$ , where  $\theta_n(\mu) = |\alpha_n^* - \alpha_\mu| + |\beta_n^* - \beta_\mu|$
- Step 4: If  $n = N - 1$ , Let  $\Gamma = \{\mu_0, \mu_1, \dots, \mu_{N-1}\}$  and stop the procedure. Else, go back to Step. 3.

Following the procedure, we can successively obtain new labelings with decreasing  $\alpha_\mu$ 's and increasing  $\beta_\mu$ 's. In Step. 1 and 3, the labeling is found according to the genetic algorithm [11] shown as Fig. 2. Firstly, a set of labelings are randomly generated as the initial population with  $P$  members. Secondly, the fitness function  $\theta(\mu)$  of each labeling in the population is evaluated and the first  $P/2$  labelings with smaller  $\theta(\mu)$ 's are kept, while the others are eliminated. Note that only  $\alpha_\mu$  and  $\beta_\mu$  of each labeling are needed to be calculated here. Then, a pair of labelings are randomly selected to carry out the crossover, where the label on each signal point of one is randomly decided with probability 0.5 whether or not to adopt the label of its mate to create an offspring. Every offspring has a probability of  $q$  to suffer a mutation, where two randomly-selected signal points on the constellation exchanges their labels. Sufficient pairs are picked until the total number of the survivors and the offsprings equals  $P$ . After that, a new iteration will start from the re-evaluation of the fitness functions. The GA will stop until  $I$  iterations have been done. Instead of BSA, GA is chosen in our design because that the randomly-generated initial population can make the search efficiency less depend on the initial labelings and that the mutation step is more likely to get the solutions out of local optimums.

Examples of the candidate sets  $\Gamma_I$  and  $\Gamma_{II}$  for SISO 16QAM are given in Table I and Table II with  $N = 6$  and 10 respectively, wherein the Gray labeling is used as the indexing of the signal points and the decimal representation is used for the binary labels. The labelings in the tables are listed in a decreasing order in terms of their  $\alpha_\mu$ 's and their corresponding curves are plotted in Fig. 3(a) and Fig. 3(b) with  $E_s/N_0 = 6$  dB at AWGN channels. Using large  $N$  is able to create a

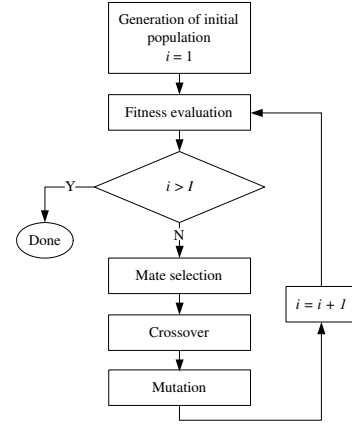


Fig. 2. A block diagram of GA.

TABLE I  
LABELINGS IN  $\Gamma_I$

$\mu$	$(\mu(0), \mu(1), \dots, \mu(15))$
$\mu_0^I$	(0,1,2,3,4,5,6,7,8,9,10,11,12,13,14,15)
$\mu_1^I$	(0,1,14,2,4,5,7,6,12,13,15,10,8,9,11,3)
$\mu_2^I$	(7,1,5,12,3,11,13,6,0,9,15,14,2,10,8,4)
$\mu_3^I$	(9,3,1,2,5,15,13,7,4,6,14,11,8,0,12,10)
$\mu_4^I$	(15,3,0,6,13,5,10,12,14,4,9,1,7,2,8,11)
$\mu_5^I$	(12,14,4,8,2,6,7,13,11,9,0,3,10,15,1,5)

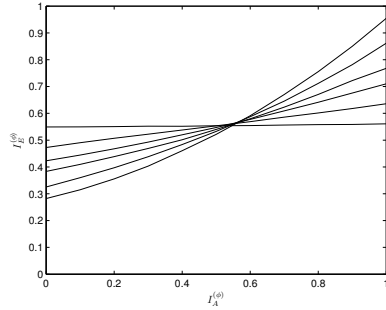
candidate set with smaller  $\delta_\alpha$  and  $\delta_\beta$ . (Note that although Gray labeling is not unique, using different Gray labelings on indexing the signal points in our tables will lead to identical set of demapper curves.) Once the SNR and the channel code are known, the labeling can then be select within  $\Gamma_I$  or  $\Gamma_{II}$  according to (6). Note that the number of labelings needed to be compared is extremely reduced from 16! (in (5)) to 6 or 10. For the MIMO case, a candidate set  $\Gamma_{III}$  for BPSK with  $N_T = N_R = 4$  on MIMO Rayleigh fading channels with  $E_s/N_0 = -1$  dB is listed with the same order in Table III and the corresponding curves are plotted in Fig. 4. The number of labelings needed to be compared is extremely reduced from 16! to 10 in  $\Gamma_{III}$ . Note that the candidate sets are obtained by setting  $I = 30$ ,  $P = 30$ , and  $q = 0.05$ . Further increasing  $I$  or  $P$  brings only trivial improvement on the minimum  $\theta_n(\mu)$  among the populations, according to our experience from experiments.

TABLE II  
LABELINGS IN  $\Gamma_{II}$

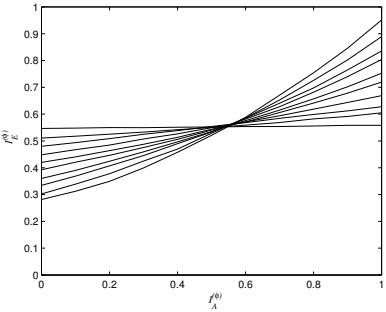
$\mu$	$(\mu(0), \mu(1), \dots, \mu(15))$
$\mu_0^{II}$	(0,1,2,3,4,5,6,7,8,9,10,11,12,13,14,15)
$\mu_1^{II}$	(0,1,2,3,4,5,6,7,8,9,15,11,12,13,10,14)
$\mu_2^{II}$	(1,4,2,6,0,5,3,7,9,8,11,10,12,13,14,15)
$\mu_3^{II}$	(1,0,2,3,4,5,14,7,8,11,10,9,12,13,6,15)
$\mu_4^{II}$	(9,15,12,14,11,1,8,2,5,4,3,6,13,7,10,0)
$\mu_5^{II}$	(12,14,4,8,2,6,7,13,11,9,0,3,10,15,1,5)
$\mu_6^{II}$	(1,13,15,5,11,9,3,12,2,4,7,0,8,14,6,10)
$\mu_7^{II}$	(5,9,15,3,0,2,6,12,8,1,4,7,10,11,14,13)
$\mu_8^{II}$	(15,11,1,2,6,8,7,4,0,9,10,3,5,12,13,14)
$\mu_9^{II}$	(4,14,9,3,7,13,10,0,2,8,15,5,1,11,12,6)

TABLE III  
LABELINGS IN  $\Gamma_{\text{III}}$

$\mu$	$(\mu(0), \mu(1), \dots, \mu(15))$
$\mu_0^{\text{III}}$	(0,1,2,3,4,5,6,7,8,9,10,11,12,13,14,15)
$\mu_1^{\text{III}}$	(8,0,2,10,4,12,6,14,1,9,3,11,5,13,7,15)
$\mu_2^{\text{III}}$	(8,0,2,10,4,12,14,6,1,9,3,11,5,13,7,15)
$\mu_3^{\text{III}}$	(1,0,2,3,4,5,7,6,9,8,11,10,12,13,14,15)
$\mu_4^{\text{III}}$	(8,4,2,10,0,12,14,6,1,9,11,3,5,13,7,15)
$\mu_5^{\text{III}}$	(1,13,6,15,5,8,2,10,4,9,3,14,0,12,7,11)
$\mu_6^{\text{III}}$	(2,13,6,9,5,8,1,15,4,10,3,14,0,12,7,11)
$\mu_7^{\text{III}}$	(0,15,7,9,5,8,10,13,4,1,3,14,2,12,6,11)
$\mu_8^{\text{III}}$	(8,15,7,9,5,0,10,13,6,1,11,14,2,12,4,3)
$\mu_9^{\text{III}}$	(15,4,0,11,2,9,13,6,1,10,14,5,12,7,3,8)



(a)



(b)

Fig. 3. The demapper transfer curves of (a)  $\Gamma_{\text{I}}$  in Table I and (b)  $\Gamma_{\text{II}}$  in Table II with  $E_s/N_0 = 6$  dB at AWGN channels.

#### IV. SIMULATION RESULTS

For SISO 16QAM, the examples of labeling selection in  $\Gamma_{\text{II}}$  are given in Fig. 5(a) and Fig. 5(b) for BCJR decoder of convolutional code with with generator matrix  $(1 + D + D^2 + D^3, 1 + D + D^3)$ , denoted by CC(17,15) for simplicity, and AWGN channels with  $E_b/N_0 = 3$  dB and 4 dB, respectively. For  $E_b/N_0 = 3$  dB, the labeling that achieves the highest first intersection is  $\mu_6^{\text{II}}$ , while for  $E_b/N_0 = 4$  dB,  $\mu_9^{\text{II}}$  becomes a favorable choice. The optimality of  $\mu_6^{\text{II}}$  and  $\mu_9^{\text{II}}$  among  $\Gamma_{\text{II}}$  for the two different SNRs can be easily verified by the BER simulation in Fig. 6, wherein a bit-interleaver of block length 80000 bits, an MAP demapper in (2) and a BCJR decoder are employed for iterative decoding with 40 iterations. It can also be observed that on one hand the labelings  $\mu_0, \mu_1, \dots, \mu_9$  which have an order of regularly decreasing  $\alpha_\mu$  can result in increasing SNRs of the occurrence of the waterfall regions and on the other hand the order of regularly increasing  $\beta_\mu$  also leads to a regularly decreasing BERs at the error floors.

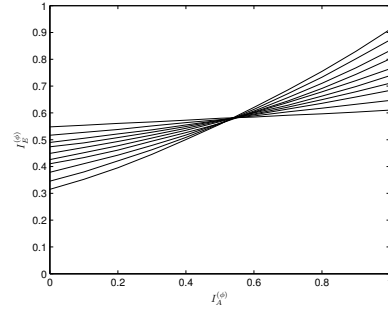
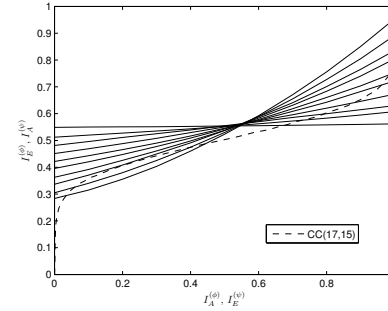
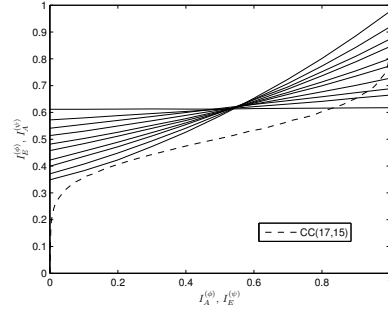


Fig. 4. The demapper transfer curves of  $\Gamma_{\text{III}}$  in Table. III with  $E_s/N_0 = -1$  dB at Rayleigh fading channels



(a)



(b)

Fig. 5. EXIT chart with the transfer curves of decoder CC(17,15) and the demapper curves in  $\Gamma_{\text{II}}$  for AWGN channels with (a)  $E_b/N_0 = 3$  dB (b)  $E_b/N_0 = 4$  dB.

Besides, each labeling is favorable at its own SNR interval and thus we can directly adopt this candidate set on different SNRs to reduce the time on re-searching a new labeling using BSA or exhaustive search. For the MIMO case, the BER simulations of labelings in  $\Gamma_{\text{III}}$  are shown in Fig. 7 for BCJR decoder of convolutional code with with generator matrix  $(1 + D + D^2, 1 + D^2)$  and Rayleigh fading channels. It can also be observed that it is beneficial to select proper labelings from  $\Gamma_{\text{III}}$  on individual SNR intervals, though the EXIT charts to illustrate the corresponding selection are omitted here due to the length limitation.

Fig. 8 shows the effect of  $N$  on the labeling selection. The labelings  $\mu_3^{\text{I}}$  and  $\mu_6^{\text{II}}$  are chosen from  $\Gamma_{\text{I}}$  ( $N = 6$ ) and  $\Gamma_{\text{II}}$  ( $N = 10$ ) respectively to achieve the highest first intersection with the decoder curve of BCJR decoder of CC(17,15), while the labeling  $\mu_C^*$  is obtained according to (5) with the help of

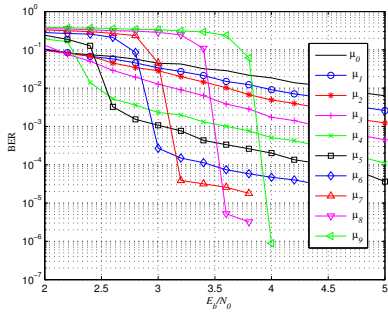


Fig. 6. The BER performance of the candidate set  $\Gamma_{II}$  for Table. II at AWGN channels.

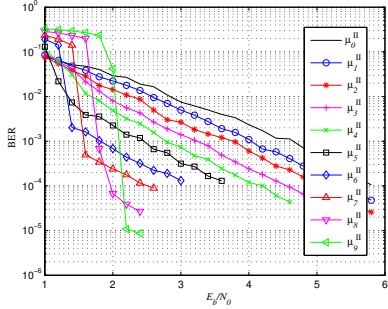


Fig. 7. The BER performance of the candidate set  $\Gamma_{III}$  for Table. III at fast Rayleigh fading channels.

GA. It is shown in Fig. 8 that  $\mu_C^*$  has the highest intersection, closely followed by  $\mu_6^II$  and then  $\mu_3^I$  at  $E_b/N_0 = 3$  dB. The corresponding BER performance in Fig. 9 sustains the observations in Fig. 8. Usually, the labeling chosen from the candidate with large  $N$  is more likely to achieve close BER performance to the BER performance of  $\mu_C^*$ . In our case,  $N = 10$  is good enough to have the close-to-optimum BER performance, while the number of labelings needed to be compared is extremely reduced to 10.

## V. CONCLUSION

A pragmatic design of labeling for MIMO BICM-ID is presented in this paper with the help of the EXIT-chart based analysis. To both reduce the search complexity and avoid trying labelings with similar shapes, the idea of the candidate set is first specified on the EXIT chart and realized by a procedure based on GA. Once the channel code and SNR are known, we can search within the candidate set for a most-suitable labeling to achieve the lowest BER with low complexity. Simulation results show that the labeling chosen from the candidate can achieve a very close BER performance to the labeling obtained by exhaustive search. Besides, even though the channel code or the SNR is changed, the same candidate set still can be directly adopted to reduce the time on re-searching new labelings using BSA or exhaustive search.

## REFERENCES

[1] A. Chindapol and J. A. Ritcey, "Design, analysis, and performance evaluation for BICM-ID with square QAM constellations in Rayleigh-fading channels", *IEEE J. Select. Areas Commun.*, vol. 19, pp. 944-957, May 2001.

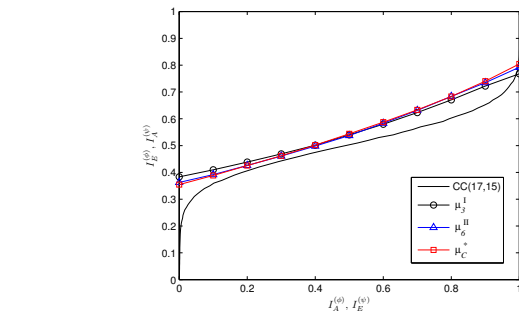


Fig. 8. EXIT chart with the transfer curves of decoder CC(17,15) and the demapper curves of labelings  $\mu_3^I$ ,  $\mu_6^II$  and  $\mu_C^*$  with  $\mu_C^* = (14, 13, 0, 4, 7, 8, 5, 1, 9, 15, 3, 10, 11, 2, 6, 12)$ .

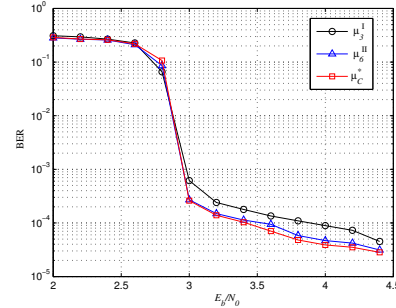


Fig. 9. The BER performance of the labelings  $\mu_3^I$ ,  $\mu_6^II$  and  $\mu_C^*$  at AWGN channels, note that the curve of  $\mu_C^*$  at  $E_b/N_0 = 3$ dB is obtained by performing 80 iterations.

[2] X. Li, A. Chindapol and J. A. Ritcey, "Bit-interleaved coded modulation with iterative decoding and 8PSK signaling," *IEEE Trans. Commun.*, vol. 50, Aug. 2002.

[3] J. Tan and G. L. Stuber, "Analysis and design of symbol mappers for iteratively decoded BICM," *IEEE Trans. Wireless Commun.*, vol 4, pp. 662-672, Mar. 2005.

[4] Q. Cheng, X. Xu, S. Zhou and L. Xiao, "A new labeling search method for bit-interleaved coded modulation with iterative decoding," in *Proc. IEEE VTC 2005-Spring Conf.*, Stockholm, Sweden, May, 2005, pp 587-590.

[5] Y. Li and X. G. Xia, "Constellation mapping for space-time matrix modulation with iterative demodulation/decoding," *IEEE Trans. Commun.*, vol. 53, pp. 764-768, May 2005.

[6] A. Sezgin and E. A. Jorswieck, "Impact of the mapping strategy on the performance of APP decoded space-time block codes," *IEEE Trans. Signal Process.*, vol. 53, pp. 4685-4690, Dec. 2005.

[7] N. H. Tran and H. H. Nguyen, "Design and performance of BICM-ID systems with hypercube constellations," *IEEE Trans. Wireless. Comm.*, vol. 5, no. 5, pp. 1169-1179, May. 2006.

[8] F. Simoens, H. Wymeersch, H. Bruneel and M. Moeneclaey, "Multi-dimensional Mapping for Bit-Interleaved Coded Modulation with BPSK/QPSK Signaling," *IEEE Comm. Lett.*, vol. 9, no. 5, May 2005.

[9] A. Ashikhmin, G. Kramer, and S. ten Brink, "Extrinsic Information Transfer Functions: Model and Erasure Channel Properties," *IEEE Trans. Inform. Theory*, vol. 50, pp. 2657-26733, Nov. 2004.

[10] T. Clevern, S. Godtmann, and P. Vary, "BER prediction using EXIT Chart for BICM with Iterative Decoding," *IEEE Comm. Lett.*, vol. 10, pp. 49-51, Jan 2006.

[11] E. K. P. Chong and S. H. Zak, *An introduction to optimization*. John Wiley and Sons, 2001.

[12] L. R. Bahl, J. Cocke, F. Jelinek and J. Raviv, "Optimal decoding of linear codes for minimizing symbol error rate," *IEEE Trans. Inform. Theory*, vol. 20, pp.284-287, Mar. 1974.